molecular pharmaceutics

Article

pubs.acs.org/molecularpharmaceutics

Vitamin D_3-Inducible Mesenchymal Stem Cell-Based Delivery of Conditionally Replicating Adenoviruses Effectively Targets Renal Cell Carcinoma and Inhibits Tumor Growth

Wan-Chi Hsiao,[†,‡] Shian-Ying Sung,[†,‡,∥] Chia-Hui Liao,[∥] Hsi-Chin Wu,[§,⊥] and Chia-Ling Hsieh*[,‡,∥,#]

[‡]Graduate Institute of Cancer Biology and [§]School of Medicine, China Medical University, Taichung 40447, Taiwan
[∥]Center for Molecular Medicine and [⊥]Department of Urology, China Medical University Hospital, Taichung 40447, Taiwan
[#]Department of Biotechnology, Asia University, Wufeng, Taichung, Taiwan

Supporting Information

ABSTRACT: Cell-based carriers were recently exploited as a tumor-targeting tool to improve systemic delivery of oncolytic viruses for cancer therapy. However, the slow clearance of carrier cells from normal organs indicates the need for a controllable system which allows viral delivery only when the carrier cells reach the tumor site. In this study, we sought to develop a pharmaceutically inducible cell-based oncolytic adenovirus delivery strategy for effective targeting and treatment of renal cell carcinoma (RCC), which is one of the most malignant tumor types with an unfavorable prognosis. Herein, we demonstrated the intrinsic tumor homing property of human bone marrow-derived mesenchymal stem cells (hMSCs) to specifically localize primary and metastatic RCC tumors after systemic administration in a clinically relevant orthotopic animal model. The platelet derived growth factor AA (PDGF-AA) secreted from RCC was identified as a chemoattractant responsible for the recruitment of hMSCs. Like endogenous osteocalcin whose barely detectable level of expression was dramatically induced by vitamin D_3, the silenced replication of human osteocalcin promoter-directed Ad-hOC-E1 oncolytic adenoviruses loaded in hMSCs was rapidly activated, and the released oncolytic adenoviruses sequentially killed cocultured RCC cells upon vitamin D_3 exposure. Moreover, the systemic treatment of RCC tumor-bearing mice with hMSC cell carriers loaded with Ad-hOC-E1 had very limited effects on tumor growth, but the loaded hMSCs combined with vitamin D_3 treatment induced effective viral delivery to RCC tumors and significant tumor regression. Therapeutic effects of hMSC-based Ad-hOC-E1 delivery were confirmed to be significantly greater than those of injection of carrier-free Ad-hOC-E1. Our results presented the first preclinical demonstration of a novel controllable cell-based gene delivery strategy that combines the advantages of tumor tropism and vitamin D_3-regulatable human osteocalcin promoter-directed gene expression of hMSCs to improve oncolytic virotherapy for advanced RCC.

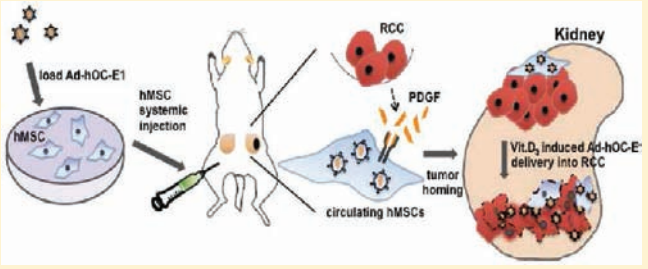

KEYWORDS: *bone marrow-derived mesenchymal stem cells, inducible cell-based gene delivery, human osteocalcin promoter, vitamin D_3, renal cell carcinoma*

INTRODUCTION

Human renal cell carcinoma (RCC) is the most common, malignant form of kidney cancer that arises from renal epithelium. Up to one-third of patients with RCC have metastases at presentation,[1] and the median survival of patients with metastatic RCC is generally less than one year.[2] Although currently available molecularly targeted therapies that inhibit activation of the vascular endothelial growth factor receptor, platelet-derived growth factor receptor (PDGFR), and the mammalian target of rapamycin pathways have shown some promise in clinical trials,[3] development of resistance to therapy and management of toxicities remain challenging. Thus, the exploration of new and effective treatment options that address the significant unmet clinical needs of patients suffering with advanced RCC merits a high priority.

Genetically engineered oncolytic adenoviruses kill cancer cells via the viral lytic replication cycle, are released, and infect adjacent cancer cells; they represent an alternative, potentially curative treatment option for metastatic RCC.[4,5] Strategies that create conditionally replicating adenoviruses with high tumor specificity take advantage of frequent mutations of the p53 pathway in tumor cells[6] or employ tumor-specific promoter elements to regulate the early viral gene, E1.[7,8] While local application of these conditionally replicating adenoviruses has provided relative success in clinical trials, imperfect tumor-specific targeting limits their clinical application as a systemic

Received: December 16, 2011
Revised: March 13, 2012
Accepted: April 5, 2012
Published: April 5, 2012

dx.doi.org/10.1021/mp200649g | *Mol. Pharmaceutics* 2012, 9, 1396−1408

therapeutic agent against cancer metastases.[9] The implementation of novel delivery strategies is needed to ensure safe delivery of efficacious oncolytic adenoviruses to locally advanced tumors and disseminated disease.

An alternative strategy for *in vivo* delivery of oncolytic viruses is using cell carriers that have inherent tumor-tropic properties and chaperone viral delivery to the tumor nodules. Bone marrow-derived mesenchymal stem cells (MSCs) are multipotent mesenchymal precursor cells that contribute to the maintenance and regeneration of a variety of connective tissues, including bone, adipose, cartilage, and muscle. MSCs are the leading candidates for tissue engineering, regenerative medicine, and autoimmune disease treatment. Circulating MSCs which integrate into and persist in the tumor stroma provide an ideal, novel platform for targeted, selective delivery of anticancer agents to invasive and metastasis tumors.[10−12] The utility of MSCs as cellular vehicles for oncolytic adenoviral therapy has shown benefits in different experimental systems in disease control.[13−16] However, ideal cellular vehicles would release oncolytic viruses only upon infiltration of tumors to avoid harmful side effects from the undesired viral spread and to maximize therapeutic viral doses at the tumor sites. The control of viral release from carrier cells has been overlooked as a research issue and needs to be addressed for further progress and clinical application.

Ligand-inducible promoters are the most prominent gene regulation system used to temporarily control exogenous gene expression for human gene therapy due to their distinct advantage of permitting pharmacological control of transgene expression after vector administration *in vivo*.[17] Vitamin D_3 (1,25-dihydroxyvitamin D_3) signals via heterodimerization of nuclear hormone vitamin D receptor with the retinoid X receptor that binds to vitamin D responsive elements (VDRE) in promoters of target genes. This vitamin D_3 cascade can be utilized to regulate transcriptional control of transgene expression using native ligands of mammalian cells, which exhibit no potential immunogenicity in humans.[5,18] Vitamin D_3 is in commonly used supplements for osteogenic induction and is involved in promoting osteocalcin (OC) production in bone-forming cells.[19] The intrinsic osteoblast-commitment property of bone marrow-derived MSCs raises the possibility that vitamin D_3 may serve as a pharmaceutical inducer of transgene expression, including the replication of oncolytic adenoviruses driven by the promoter of human OC gene[5,18] in MSC cells.

In the present study, we hypothesized that the RCC tumor-tropic property of human MSCs (hMSCs) would be greater than that of differentiated bone stromal cells. We assessed various RCC-derived chemoattractants for hMSC migration. We hypothesized that the endogenous and ectopic OC promoter would be normally silenced in hMSCs but could be highly activated by vitamin D_3. We also hypothesized that hMSC-based delivery of vitamin D_3-inducible oncolytic adenoviruses would provide an RCC-targeted gene therapy strategy for the systemic treatment of human RCC tumors in a clinically relevant, orthotopic tumor model. The efficacy of pharmaceutically controlled replication of oncolytic adenoviruses in MSC cellular vehicles could be easily translated to the clinical setting.

MATERIALS AND METHODS

Cell Lines and Cell Culture. Established RCC human cell lines[5] were grown in Dulbecco's modified Eagle's medium (DMEM) supplemented with 10% fetal bovine serum and 1% penicillin-streptomycin (Invitrogen, Carlsbad, CA). Bone marrow stromal cell line HS27A was obtained from ATCC (Manassas, VA) and grown in the same medium as RCC cells. Human bone marrow-derived mesenchymal stem cells (hMSC) and normal human renal epithelial cells (HRE) purchased from Lonza (Rockland, ME) were maintained in mesenchymal stem cell medium and renal epithelial cell growth medium, respectively, according to the manufacturer's instructions (Lonza). To avoid the possible variability of cultured hMSC because of increased differentiation during later cell passages *in vitro*, only hMSCs from passage numbers below 15 were used. Human MSC cells were routinely tested for stem cell properties by a surface antigen expression pattern and multilineage differentiative ability following manufacturer's guidelines. The HEK 293A cell line, which was used for production, amplification, and titering of recombinant adenoviruses (Invitrogen), was maintained in DMEM supplemented with 10% fetal bovine serum (FBS), 0.1 mM MEM non-essential amino acids, 2 mM L-glutamine, and 1% penicillin/streptomycin. To generate luciferase- and enhanced green fluorescent protein (EGFP)-expressing RCC cell lines (RCC-Luc and RCC-GFP, respectively), RCC cells were stably transduced with a lentiviral vector containing firefly luciferase or EGFP cDNA, which was constructed using the ViralPower Lentiviral Gateway Expression System from Invitrogen. All cells were maintained in a humidified incubator at 37 °C with 5% CO_2.

Reagents and Adenoviral Vectors. Vitamin D_3 analogue (Ro 25-9022) was provided by Roche (Nutley, NJ). Ethanol was used as the vehicle control for the vitamin D_3 analogue. The adenoviruses, Ad-CMV-EGFP and Ad-hOC-E1, were previously produced and described.[18,20] Ad-CMV-EGFP, a replication-defective adenovirus, expresses EGFP under the control of a cytomegalovirus (CMV) major immediate-early promoter. Ad-hOC-E1 is a conditional replication-competent adenovirus containing a single bidirectional 800-bp human OC promoter to drive both early viral *E1A* and *E1B* genes.

Real-Time Quantitative PCR (RT-PCR). Cells were treated with a 5 nM vitamin D_3 analogue or ethanol vehicle control for 48 h and then subjected to RNA extraction using the RNeasy Mini kit from QIAGEN (Valencia, CA). cDNA was synthesized from 1 μg of total RNA annealed with random primers and reverse-transcribed with MMLV reverse transcriptase (Invitrogen). Quantitative RT-PCR was performed using the LightCycler 480 TaqMan master kit with gene-specific primers and the corresponding Universal Probe Library probe (Roche Applied Science, Mannheim, Germany). Primer and probe sequences (5′→3′) used to amplify and detect the transcript were as follows: human OC (Forward: tgagagccctcacactcctc, Reverse: acctttgctggactctgcac, Probe 81), human PDGFRα (Forward: aggtggttgaccttcaatgg, Reverse: tttgatttcttccagcattgtg, Probe 80), and housekeeping gene heat shock 90kD protein 1, beta (HSPCB) (Forward: agcctacgttgcactattacg, Reverse: gaaaggcaaaagtctccacct, Probe 55). Real-time PCR reactions and data analyses were conducted as described previously.[21] Relative gene expression in each group was represented as $2^{-\Delta CT}$, where ΔCT is determined by subtracting the average HSPCB CT value from the average target gene value.

Cytokine Antibody Array and Enzyme-Linked Immunosorbent Assay (ELISA). Human cytokine antibody array C Series 2000 kit was used according to the manufacturer's instructions (RayBiotech, Norcross, GA). Briefly, the array membrane coated with cytokine-specific antibodies was blocked

with blocking buffer and then incubated with 1.5 mL of the serum-free conditioned medium collected from HRE and RCC42 cells for 2 h. The unspecific bound proteins were washed out, and the membranes were incubated with a diluted cocktail of biotinylated antibodies for 2 h. The membrane was washed, incubated with peroxidase-labeled streptavidin for 2 h at room temperature (r.t.), and developed using enhanced chemiluminescence solution. Signals were captured on X-ray films, and dot intensities of different cytokines were quantified by densitometry using ImageJ software and values normalized to the intensity of internal positive controls. Concentration of platelet derived growth factor AA (PDGF-AA) in conditioned medium was quantified using the human PDGF-AA Quantikin ELISA Kit (R&D Systems, Minneapolis, MN) according to the manufacturer's instructions.

Transfection and Luciferase Reporter Assay. Cells were plated into 6-well plates in triplicates and transfected with phOC-Luc, a previously generated hOC promoter-driven luciferase reporter plasmid[22] using Lipofectamin 2000 reagent (Invitrogen). The pRL-TK plasmid (Promega, Madison, WI) that expresses Renilla luciferase was cotransfected to normalize for transfection efficiency. After transfection, cells were treated with 5 nM vitamin D_3 or ethanol vehicle control for 48 h and then subjected to luciferase activity assay with the dual-luciferase assay system (Promega) according to the manufacturer's protocol. The relative luciferase activity was calculated by dividing the firefly luciferase relative light units (RLU) by the RLU values obtained for the Renilla luciferase.

***In Vitro* Migration Assay.** The migration of hMSC toward RCC cells was assessed using 24-well transwell plates (Millipore, Bedford, MA). To distinguish the migrated cells, hMSC and HS27A cells were labeled with Vybrant CFDA-SE (carboxyfluorescein diacetate succinimidyl ester) cell tracer (Invitrogen) prior to the migration assay according to the manufacturer's protocol. For the migration assay, 10^5 RCC cells or HRE cells were grown in the lower chamber of transwells under the low serum (1% FBS) condition. After 48 h of incubation, 10^5 CFDA-SE labeled hMSCs or HS27A cells in 200 μL of serum-free RPMI medium were added to the upper chamber containing 8-μm pore polycarbonate. Cells that migrated through the membrane were counted 3 h after cell plating under a Zeiss Axiovert 200 fluorescent microscope (Carl Zeiss MicroImaging, Thornwood, NY) with a 10× objective. Each experiment was independently performed at least twice in triplicate.

***In Vitro* Cytotoxicity Assay.** For virus-mediated cytotoxicity, 2×10^4 RCC or hMSC cells were seeded onto 24-well plates for 16 h. Cells were infected with adenoviral vectors at a range of multiplicity of infection (moi) for 2 h, and media were replaced. After 24 h, cells were incubated with 5 μM vitamin D_3- or ethanol-containing medium for 7 days, and the viable cells were detected by 0.2% crystal violet staining. For hMSC-delivered viral cytotoxicity, RCC cells (10^4/well) were seeded in 24-well plates and allowed to attach for 6 h. Human MSCs that were preinfected with 1000 moi of adenoviral vectors were added to each well containing RCC cells in a ratio of 1:3 and 1:1. Cocultured cells were exposed to 5 nM vitamin D_3 or ethanol for 7 days and subjected to crystal violet staining.

Animal Studies. Institutional guidelines and an Animal Research Committee-approved protocol were followed for the mouse studies. Six-week-old male BALB/c nude mice were purchased from BioLASCO Taiwan Co. (Taipei, Taiwan). To establish an orthotopic RCC tumor model, 5×10^5 RCC-EGFP (for hMSC tumor tropism) or RCC-Luc (for therapeutic intervention) were resuspended in 20 μL of PBS and injected into the subrenal capsule of the left kidney of anesthetized mice by using a 0.5 mL syringe with 27-gauge needle. After 14 days of tumor development, mice received one of the following treatments: For evaluation of hMSC migration toward RCC tumors, hMSCs were transduced with the luciferase gene using an Ad-CMV-Luc vector at an moi of 1000. One day after infection, 1×10^5 of the resultant hMSCs (hMSC-Luc) in 100 μL of PBS were intraperitoneally (i.p.) administered into tumor-bearing mice and sham-operated mice (n = 5 in each group). The hMSC-Luc cell trafficking was real-time monitored daily by bioluminescence imaging with the IVIS spectrum imaging system (Xenogen Corp, CA) as described previously.[21] Six days after hMSC-Luc injection, all animals were sacrificed, and organs were excised for *ex vivo* bioluminescence imaging analysis. Fluorescence imaging was performed with an excitation of 465 nm and an emission of 520 nm wavelengths. Acquired data were analyzed using Living Image 4.0 software.

For evaluation of the efficacy of MSC delivered, vitamin D_3 controlled, oncolytic tumor therapy, two weeks after RCC-Luc cells injection, RCC-Luc tumor-bearing mice were randomized and received an i.p. injection of 2×10^5 hMSC cells that had been infected with 1000 moi (2×10^8 total infectious virus particles) of Ad-hOC-E1 or Ad-CMV-EGFP for 4 h and resuspended in 100 μL of PBS after washing. Six days after hMSC injection, mice (n = 5) received i.p. administration of 100 μL of vitamin D_3 (2 ng/dose) or oil vesicle (3.2% ethanol, 2.6% PEG-400, 2.2% Tween 80, and 92% PBS) twice per week for 4 weeks (Figure 6A). One control group received no treatments. A second control group was administered 2×10^8 plaque formation unit (pfu) of carrier-free Ad-hOC-E1 (100 μL) i.p. and the aforementioned vitamin D_3 treatment. Tumor growth was monitored weekly by bioluminescence imaging. Mice were sacrificed 6 weeks after treatment, and tumors were dissected, weighed, embedded in paraffin, and subjected to histopathologic examination.

Immunofluorescent Staining. RCC-GFP tumor tissues were harvested from mice 6 days after hMSC-Luc cells administration using the standard protocol, frozen, and sliced into 5 μm thick sections on a Leica CM1850 cryostat (Leica Microsystems, Wetzlar, Germany). Slides were incubated with goat polyclonal antiluciferase (1:1000, Rockland, Gilbertsville, PA) and rabbit polyclonal anti-GFP (1:200, GeneTex, San Antonio, TX) at r.t. in a moist chamber for 2 h. After washing for 30 min in PBS, sections were incubated for an additional 1 h with Alexa Fluor 546-conjugated donkey antigoat IgG (Invitrogen) and Alexa Fluor 488-conjugated donkey antirabbit IgG (Invitrogen) in a 1:200 dilution at r.t. and counterstained with 4′,6-diamino-2-phenylindole (DAPI; Sigma, St. Louis, MO) to visualize nuclei. Fluorescence images were acquired using a Zeiss Axiovert 200 M fluorescent microscope (Carl Zeiss Microimaging) with a 40× objective.

Immunohistochemistry. Paraffin-embedded sections from mouse tumors collected at 6 weeks after therapy (end of efficacy experiments) were deparaffinized and rehydrated using xylene and decreasing concentrations of ethanol. Adenoviral hexon protein was detected in tumor xenografts using a Novolink polymer detection system (Leica Microsystems, Newcastle Upon Tyne, U.K.) following the kit instructions. Briefly, antigen retrieval was performed with a steamer by heating the slides in 10 mM sodium citrate buffer (pH 6.0) for 10 min. Slides were incubated with goat polyclonal

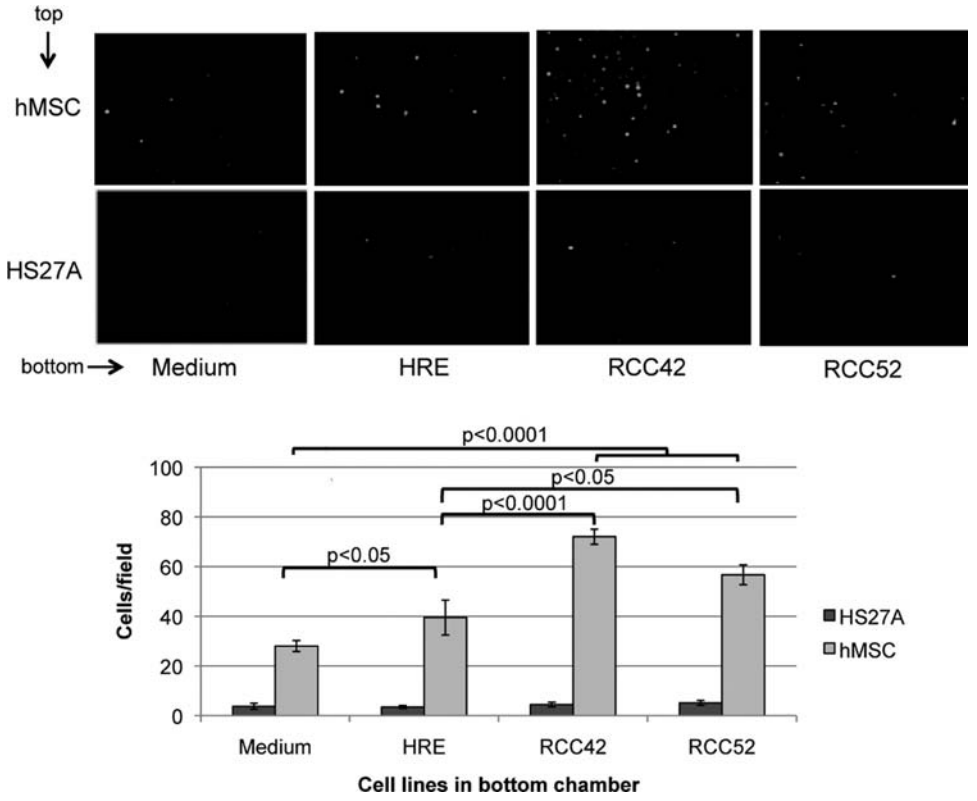

Figure 1. Migratory response of hMSCs and differentiated HS27A bone stromal cells to normal and malignant renal epithelial cells. (A) Representative photographs of migrated CFDA-labeled hMSC or HS27A cells toward the medium, normal renal epithelial cells (HRE) and RCC cells at the bottom chamber of transwells. Fluorescent images were captured at 3 h after plating cells by using an X10 objective. (B) Quantification of migration of cells from a transwell migration assay: fluorescent cells in the bottom chamber were counted under a fluorescent microscope. Data are represented as the average number of migrated cells per high-power field (means ± SD) for each condition in triplicate wells counted in quadruplicate fields.

antiadenovirus (1:1000, AB1056; Millipore) at r.t. for 1 h, washed, and incubated with HRP-polymer conjugate under the same conditions. Peroxidase activity was developed with diaminobenzidine for 5 min, and slides were counterstained with hematoxylin. Apoptosis was evaluated using the Apo-BrdU-IHC in situ DNA fragmentation assay kit (BioVision, Inc., Mountain View, CA) as described previously.[5]

Statistical Analysis. For the *in vitro* studies, all data are presented as the mean ± SD unless otherwise specified. Differences between groups were analyzed using the two-tailed, unpaired Student's *t*-test. A *p*-value of less than 0.05 was defined as significant. In the mouse studies, the impaired Mann−Whitney test was used for group comparison.

RESULTS

Human MSC Cells Preferentially Migrated toward RCC. To investigate the potential use of hMSCs as cellular carriers for RCC tumor targeting, we first examined the migratory ability of hMSCs toward RCC cells in an *in vitro* coculture cell model in which human normal HRE, malignant RCC cells, or plain culture medium were placed on the bottom chamber of transwells and hMSCs were seeded on the top chamber. After 3 h incubation, significantly higher numbers of hMSCs were recovered from the lower chamber where RCC42 and RCC52 were present compared with a medium control (Figure 1, 72 ± 3.5 and 56.7 ± 4.2 per field versus 28 ± 1.4 cells; $p < 0.0001$). However, HRE seeded on the bottom chamber showed only a minor effect on attracting hMSC migration (39.5 ± 6.7 per field). In a parallel study, hMSCs were replaced with differentiated HS27A bone marrow stromal cells to address whether RCC tumor tropism is cell context-specific. Unlike hMSCs, HS27A barely responded to the chemoattractive cue sent from RCC cells, and only a limited number of cells moved toward the bottom chamber with no significant difference compared with the normal HRE or plain medium control ($p > 0.5$). These results suggested that bone marrow-derived MSC, but not differentiated stromal cells, have a unique propensity to migrate toward RCC.

To determine whether hMSCs are capable of integrating into the tumor site of human RCC after systemic delivery, an orthotopic RCC xenograft tumor model was established by injecting RCC-GFP cells into the kidney capsule of nude mice. Once tumors were established, sham and tumor-bearing mice received hMSC-Luc cells by i.p. injection. The fate of hMSC-Luc cells in mice was monitored by bioluminescence imaging daily up to 6 days. Kinetics data showed that bioluminescent signals had begun to migrate toward the site of the affected kidney capsule within 3 days after cell injection in both tumor-bearing and sham-operated animals (Figure 2A). However, while the signal had disappeared by day 4 postadministration in sham-operated mice, light emission was sustained in tumor-bearing mice for at least 6 days. Notably, a few mice with RCC xenografts had additional bioluminescence signals shown in the lower abdomen (Figure 2A, bottom panel) on day 4, which suggested that RCC tumor cells had formed distant metastases. In addition, i.p. administrated HS27A-Luc cells, which barely migrated toward cocultured RCC cells *in vitro* (Figure 1), failed

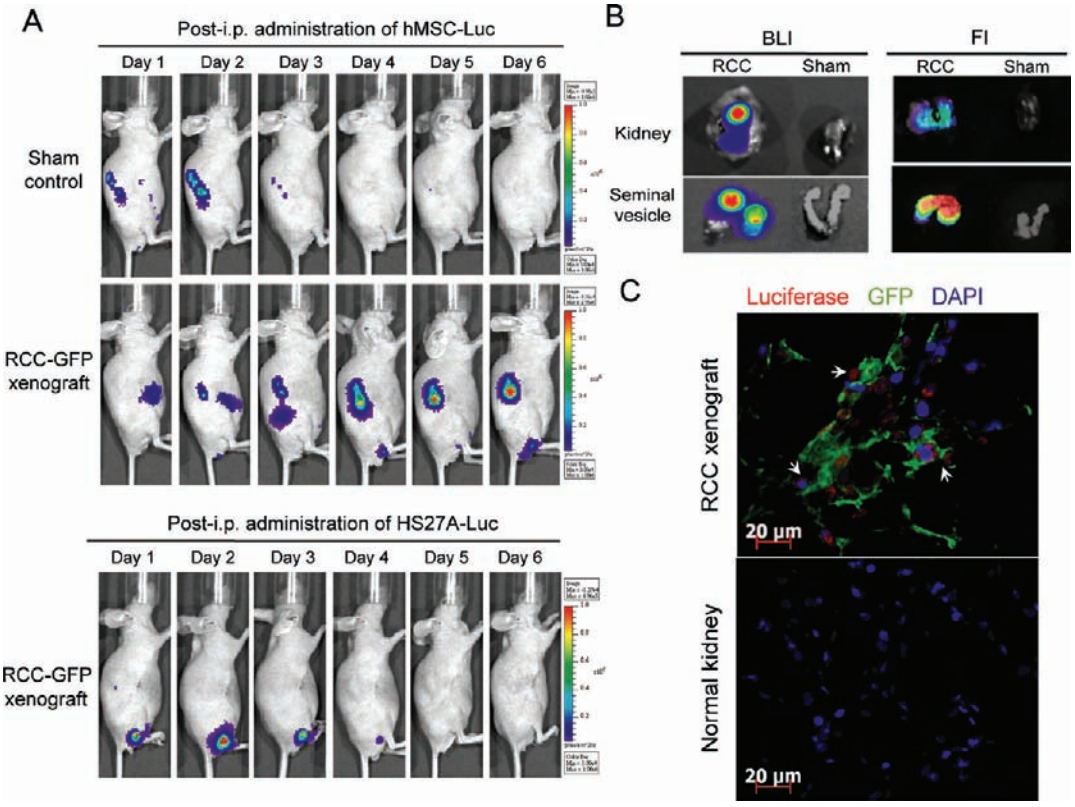

Figure 2. Homing of systemically administered hMSCs to the sites of RCC tumors. (A) Kinetics and distribution of systemically administered hMSC or HS27A. Whole-body bioluminescent images were obtained from representative nude mice that carried orthotopic RCC-GFP xenografts or received sham operation (sham control) at the indicated time points after i.p. administration of luciferase-expressing hMSC (hMSC-Luc) or HS27A (HS27A-Luc) cells. (B) Representative bioluminescent images (BLI) of mouse kidney and seminal vesicle excised from RCC-GFP tumor-bearing mice and sham-operated mice that received hMSC-Luc administration and the same organs imaged with the configurable filters for green fluorescence (FI, right panel). (C) Immunohistochemical examination of administered hMSC-Luc infiltration into the RCC tumor microenvironment. Representative sections from RCC-GFP xenografts in mice kidneys (upper panel) and normal kidney counterparts from sham-operated mice (lower panel) stained with a fluorescenceconjugated antiluciferase antibody revealed the distribution of hMSC-Luc (red) cells within the RCC-GFP xenograft (green). All nuclei were counterstained with DAPI (blue).

to be recruited to RCC tumor sites, confirming the cell-specific capacity of hMSC to localize RCC tumors.

To localize the origin of the luminescence, we isolated organs from the mice and reimaged them on day 6 of the hMSC-Luc injection. The signals at the site near surgical operation were confirmed as tumor-bearing kidneys, and the signal detected in the lower abdomen was found to originate from the seminal vesicle (Figure 2B, upper panel). Organs that showed positive for luminescence imaging also exhibited strong signals of green fluorescence that reflected the presence of RCC-GFP cells (Figure 2B, lower panel). In contrast, no light, either luminescence or green fluorescence, was emitted from the kidney and seminal vesicle collected from sham-operated mice, confirming the tumor-homing ability of hMSCs to primary and metastatic RCC tumors. The infiltration of hMSC-Luc into tumor microenvironments was further validated by immunofluorescence staining of tumor sections with antiluciferase antibodies, which detected transplanted hMSC-Luc cells. Fluorescent microscopy (Figure 2C) revealed hMSC-Luc cells (red) throughout the RCC-GFP xenografts (green) after i.p. injection, whereas no hMSC-Luc cells were detected in kidney sections from sham-operated mice.

PDGF-AA Involved in the RCC Conditioned Medium-Induced hMSC Migration. To identify the chemoattractive factors that promoted the migration of hMSCs by RCC cells, human cytokine antibody arrays were used to compare the cytokine expression profile of conditioned medium collected from normal HRE and malignant RCC42 cells, a representative RCC cell line. Among 174 cytokines were tested, one sole cytokine, PDGF-AA, was significantly higher in RCC42 cells compared with HRE (Figure 3A). Consistent with the array observation, quantitative data obtained from ELISA assay revealed that the conditioned medium of RCC42 had a greater than 10-fold higher concentration of PDGF-AA (1120 pg/mL) than that of HRE (90 pg/mL). To exclude the possibility that greater PDGF-AA production in RCC42 than that of normal HRE is cell line-specific rather than RCC-specific, we examined the mRNA level of PDGF-A in a panel of human RCC cell lines. All (5/5) tested RCC cell lines yielded higher amounts of RT-PCR product of PDGF-A than HRE (Supporting Information, Figure S1A), confirming elevated expression of PDGF-AA in RCC cells. On the other hand, the α subunit of PDGFR-$\alpha\alpha$, the receptor for PDGF-AA, was significantly expressed by hMSCs but was barely detectable in HS-27A cells (Supporting Information, Figures S1B and C), which exhibited low chemotactic ability to RCC cells.

To determine whether PDGF-AA is responsible for the RCC conditioned medium-induced hMSC migration, we first examined the effect of purified human recombinant PDGF-AA (rPDGF-AA) on the chemoattraction of hMSCs. A cell migration assay was performed with the addition of rPDGF-AA into the serum-free medium in the bottom chamber of the

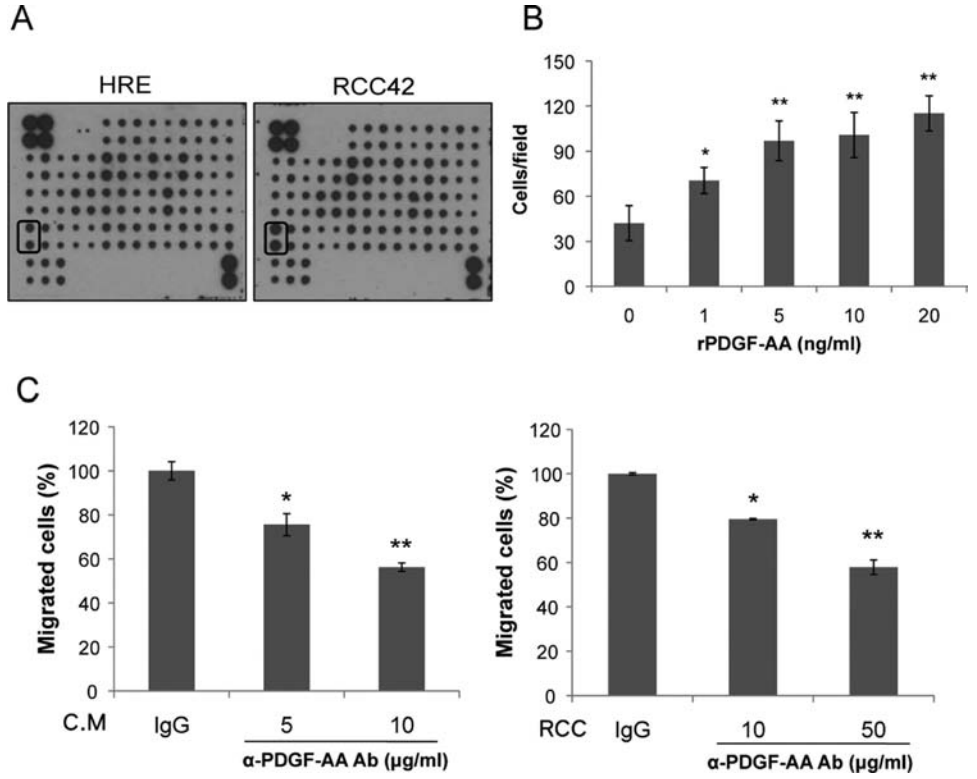

Figure 3. Involvement of PDGF-AA in RCC-mediated hMSC migration. (A) Cytokine expression profile of the conditioned medium obtained from HRE and RCC42 cell lines. Cytokine production was analyzed by using the human cytokine antibody Array C Series 2000, and the autoradiograph of one set of Array VIII containing PDGF-AA spots (rectangle boxes) was presented. (B) Chemotactic response of hMSCs induced by human recombinant PDGF-AA (rPDGF-AA) at the indicated concentration. Data are represented as mean ± SD of the number of cells per high-power field of three separate experiments carried out in duplicate. *$P < 0.05$, **$P < 0.005$ versus serum-free medium alone (0 μg/mL rPDGF-AA). (C) Inhibition of hMSC cell migration to either conditioned media or RCC cells by anti-PDGF-AA antibody. Conditioned media (CM) from RCC42 cells (left panel) or RCC42 cells grown at the bottom chamber of transwells (right panel) were mixed with the indicated concentration of mouse anti-PDGF-AA antibody. Treatment with 10 μg/mL or 50 μg/mL of mouse IgG (IgG) was a negative control, respectively, and set as 100%. Values are means ± SD of three independent experiments *, $P < 0.05$, **, $P < 0.005$ vs mouse IgG.

transwell. Higher numbers of hMSCs migrated through the membrane in a PDGF-AA dose-dependent manner with the plateau at the concentration of 5 ng/mL (Figure 3B). The role of PDGF-AA in the conditioned medium of RCC cells on the induction of hMSC migration was elucidated by treating RCC conditioned medium with a PDGF-AA neutralizing antibody. As shown in Figure 3C, the migration of hMSCs was inhibited by 25% and 45% when a PDGF-AA-specific antibody was present at the concentrations of 5 μg/mL and 10 μg/mL, respectively. A similar result was obtained in the coculture system where incubation of RCC42 cells with PDGF-AA neutralizing antibody at the bottom chamber of transwells decreased the number of migrated hMSCs in a dose-dependent manner (Figure 3C, left panel). Moreover, the knockdown of PDGF-AA in RCC cells by stable transfection of cells with a lentivirus-mediated short hairpin RNA (shRNA) reduced the ability of RCC cells in attraction of hMSCs migration and homing to tumor sites (Supporting Information, Figure S2). Taken together, these results suggested that RCC-induced chemotaxis of hMSC cells is at least in part mediated by PDGF-AA.

Vitamin D_3 Extensively Induced Human Osteocalcin Promoter Activity in hMSCs. We have previously demonstrated the feasibility of vitamin D_3 in the induction of human osteocalcin (hOC) promoter-mediated transgene expression in RCC cells.[5] To test the potential utility of this vitamin D_3-dependent inducible expression system to precisely regulate transgene expression levels between the extremes of suboptimal and supraoptimal thresholds in hMSC cell carriers, we first determined the basal and vitamin D_3-induced OC gene expression by quantitative RT-PCR (Figure 4A). Unlike osteoblast MG63 cells that consistently expressed a high level of OC, the basal level of OC mRNA was extremely low in hMSCs with a threshold cycle between 32 and 33 compared to 21 for the housekeeping gene HSPCB. However, the addition of vitamin D_3 increased expression of OC approximately 500-fold in hMSCs, where the expression level was greater than that in MG63 cells. Consistent with endogenous OC gene expression, luciferase transgene driven by an ectopic hOC promoter containing VDRE motif was barely detected in hMSCs under normal culture conditions, and vitamin D_3 increased the rate approximately 35-fold (Figure 4B). Moreover, treatment of hMSCs with either a replication-defective Ad-CMV-EGFP adenoviral vector or an oncolytic Ad-hOC-E1 adenovirus whose replication is directed by hOC promoter was unable to cause any cell death, even at the moi as high as 1000 (Figure 4C), a viral dose two times higher than that sufficient to infect 100% of hMSCs (Supporting Information, Figure S3). However, despite vitamin D_3-induced cell differentiation and inhibitory effect on hMSC proliferation, further vitamin D_3-induced cytotoxicity was observed in cells that were infected with Ad-hOC-E1, but not Ad-CMV-EGFP, in a viral dose-dependent manner. These results suggest that the vitamin D_3-dependent, hOC promoter transcription-regulated system is

dx.doi.org/10.1021/mp200649g | Mol. Pharmaceutics 2012, 9, 1396–1408

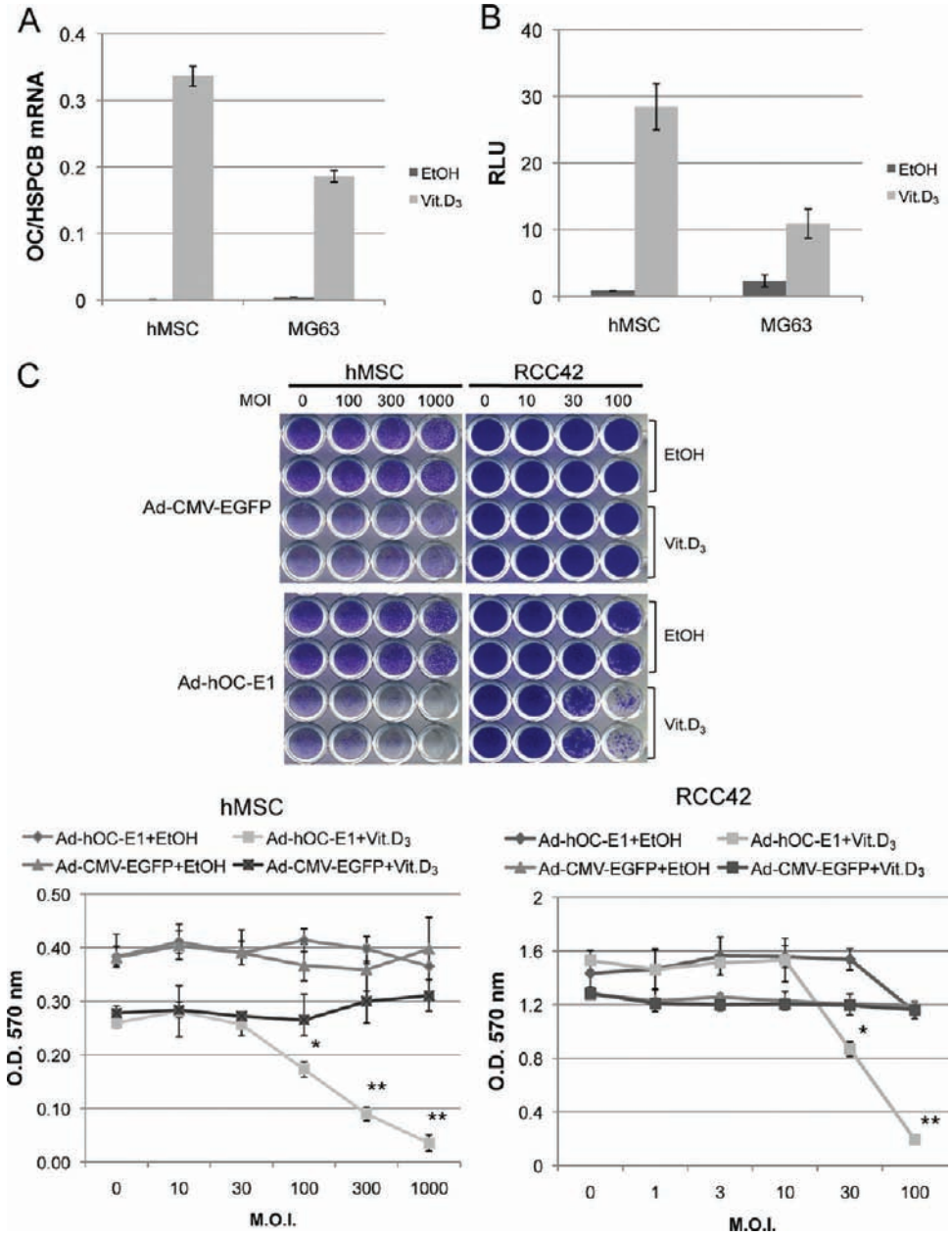

Figure 4. Effect of vitamin D_3 on human osteocalcin promoter-directed transgene expression. (A) Basal and vitamin D_3-induced OC mRNA expression in RCC and hMSC cell lines. Cells were either maintained under control conditions (EtOH) or treated with 5 nM vitamin D_3 (Vit. D_3) for 48 h and subjected to qRT-PCR. The MG63 osteosarcoma cell line was used as a positive control for vitamin D_3 action. Human OC gene expression was normalized to HSPCB and presented as means ± SD of three independent experiments. (B) Induction of hOC promoter activity by vitamin D_3. Dual luciferase assay of hOC promoter activity after cotransfection into hMSCs and MG63 cells with an expression plasmid, phOC-Luc, and an internal control plasmid, pRL-TK, in the presence or absence of 5 nM vitamin D_3 48 h after transfection. The data are presented as a ratio of firefly to Renilla luciferase activity and represented an average of three independent experiments. (C) hMSCs and RCC42 cells were infected with Ad-hOC-E1 or Ad-CMV-EGFP at indicated doses and then subjected to 5 nM vitamin D_3 or vehicle control treatment for 7 days. Cell viability was determined by crystal violet staining that was photographed (upper panel). The relative cell number was quantified by determining optical absorbance at 570 nm. Data are presented as the mean ± SD of three independent experiments (bottom panel). *, $P < 0.05$; **, $P < 0.001$ vs uninfected control (moi = 0).

suitable to regulate the timing and level of expression on early E1 genes of adenovirus in hMSC cells.

Ad-hOC-E1-Loaded hMSC Exerted Oncolytic Effect on Cocultured RCC Cells upon Vitamin D_3 Stimulation. To determine whether Ad-hOC-E1 replicated within hMSCs and the released virions were able to infect and kill neighboring RCC cells and subsequently kill both cellular components, RCC cells were cocultured with increasing numbers of the Ad-hOC-E1-loaded hMSCs in the presence or absence of vitamin D3. To exclude any toxic effects of the adenovirus infection itself that may also contribute to cell lysis, tumor cells were also mixed with hMSC carrier cells infected with replication-defective Ad-CMV-EGFP virus. Crystal violet staining of viable cells 7 days after coculture revealed a vitamin D_3-dependent cytotoxicity of cocultured RCC and Ad-hOC-E1-loaded hMSCs, which caused a 70−95% cytolysis in a dose-dependent

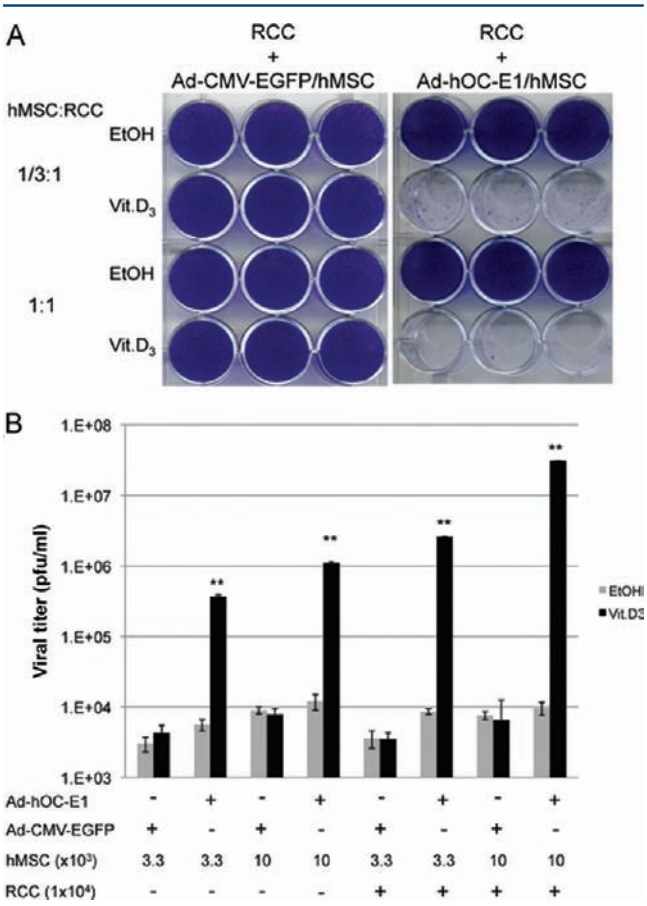

Figure 5. Cytotoxicity of hMSC-delivered Ad vectors in cocultured RCC cells. hMSCs were preinfected with Ad-hOC-E1 or replication defective Ad-CMV-EGFP control vector at 1000 moi for 24 h and subjected to cultivation with a fixed number (1×10^4) of RCC cells at a hMSC/RCC ratio of 1:3 or 1:1 in the presence or absence of vitamin D_3. (A) The cytopathic effect was observed by crystal violet staining at 7 days after coculture and photographed. (B) The viral titer of culture supernatants harvested from hMSC viral carriers alone or cocultured with RCC cells was determined by plaque assay and expressed as the average number of plaque forming units per milliliter (pfu/mL). **, $P < 0.001$ vs the vehicle control (EtOH) group.

manner (Figure 5A). No cytopathic effect was observed in mixed cultures of RCC and Ad-CMV-EGFP-loaded hMSC at any combination ratio, regardless of the presence of vitamin D_3.

To assess whether the cytotoxicity of cocultured RCC cells caused by Ad-hOC-E1-loaded hMSC plus vitamin D_3 treatment resulted from a boosted viral production, we collected culture medium from each testing group and performed a plaque assay using 293A cells. As shown in Figure 5B, Ad-hOC-E1-loaded hMSCs monoculture or cocultured with RCC cells in the absence of vitamin D_3 exhibited a viral titer similar to that of replication-defective Ad-CMV-EGFP-loaded hMSCs, indicating that some of the original inoculums remained but no denovo viruses were produced under this condition. However, vitamin D_3 treatment increased the viral titer of Ad-hOC-E1 approximately 100 fold, which indicated completion of viral replication in infected hMSC cells. As RCC cells were susceptible to Ad-hOC-E1 viral infection and replication upon vitamin D_3 induction (Figure 4C),[5,18] the levels of vitamin D_3-dependent viral production shown in the monoculture of Ad-hOC-E1-infected hMSCs were significantly enhanced by more than one log when additional RCC cells were present in the culture. Taken together, these results indicated that vitamin D_3 initiated Ad-hOC-E1 viral replication in hMSC carrier cells which released infectious progeny viruses to neighboring RCC cells for further amplification and cytotoxicity.

Systemic Administration of Ad-hOC-E1-Loaded hMSCs Followed by Vitamin D_3 Inhibited the Growth of RCC Tumors. We next determined whether the systemic administration of Ad-hOC-E1-loaded hMSCs combined with follow-up vitamin D_3 treatment could effectively deliver virus to RCC tumors and improve the therapeutic effect over carrier-free viral injection. To noninvasively monitor the tumor growth in the kidneys, RCC cells were stably transduced with a luciferase reporter gene and injected into the capsule of kidney. When orthotopic RCC tumors were established, as determined by luciferase imaging, tumor-bearing mice were randomly divided into six groups for different treatment: a no-treatment control (untreated) group, i.p. administration of Ad-hOC-E1- or Ad-CMV-EGFP-loaded hMSCs combined with vitamin D_3 or oil vesicle, and i.p. injection of carrier-free Ad-hOC-E1 viruses combined with subsequent vitamin D_3 (Figure 6A). Based on the bioluminescent imaging data (Figure 6B), RCC xenografts were very aggressive tumors that progressed rapidly with an average 200-fold increase of bioluminescence light emission over a four-week period. Normalized signal progression levels (tumor growth) increased to a similar extent despite i.p. administration of Ad-CMV-EGFP-loaded hMSCs, either combined with or without vitamin D_3, suggesting no therapeutic inhibition with these agents. While combination treatment with carrier-free Ad-hOC-E1 viral i.p. injection and vitamin D_3 caused a mild delayed progression (~95-fold increase) of photonic emissions, Ad-hOC-E1-loaded hMSCs combined with vitamin D_3 treatment maintained a relatively constant or slowly changing profile of bioluminescence signals over time with an average 35-fold increased activity at week 5 after tumor cell inoculation. A comparison of the efficacy of the delivery methods indicated that Ad-hOC-E1-directed tumor growth inhibition was much more effective delivered in hMSCs than that by conventional i.p. viral injection.

To better characterize the therapeutic effect of inducible hMSC-based oncolytic virotherapy, we excised tumors from all mice after 6 weeks of treatment and assessed the tumor burden. As shown in Figure 6C, no significant changes were observed in the average tumor weight of animals that received no treatment or received Ad-CMV-EGFP-loaded hMSCs single treatment or combined with vitamin D_3. Consistent with our previous findings in the subcutaneous RCC xenograft model that concomitant carrier-free Ad-hOC-E1 virotherapy and vitamin D_3 have beneficial effects on tumor regression,[5] i.p. administered carrier-free Ad-hOC-E1 virotherapy and vitamin D_3 reduced the tumor weight by 20%, as expected for the viral dose used herein. However, mice that underwent the same treatment protocol but received Ad-hOC-E1 viruses delivered using hMSC carriers showed prominent tumor inhibition to be less than 45% of the untreated control. We also found that hMSC-delivered Ad-hOC-E1 monotherapy caused slightly but not significantly decreased tumor weight. This minor tumor inhibition might be due to the effects of endogenous vitamin D_3 on the induction of sublethal dose of viruses releasing from hMSC carrier cells.

dx.doi.org/10.1021/mp200649g | Mol. Pharmaceutics 2012, 9, 1396–1408

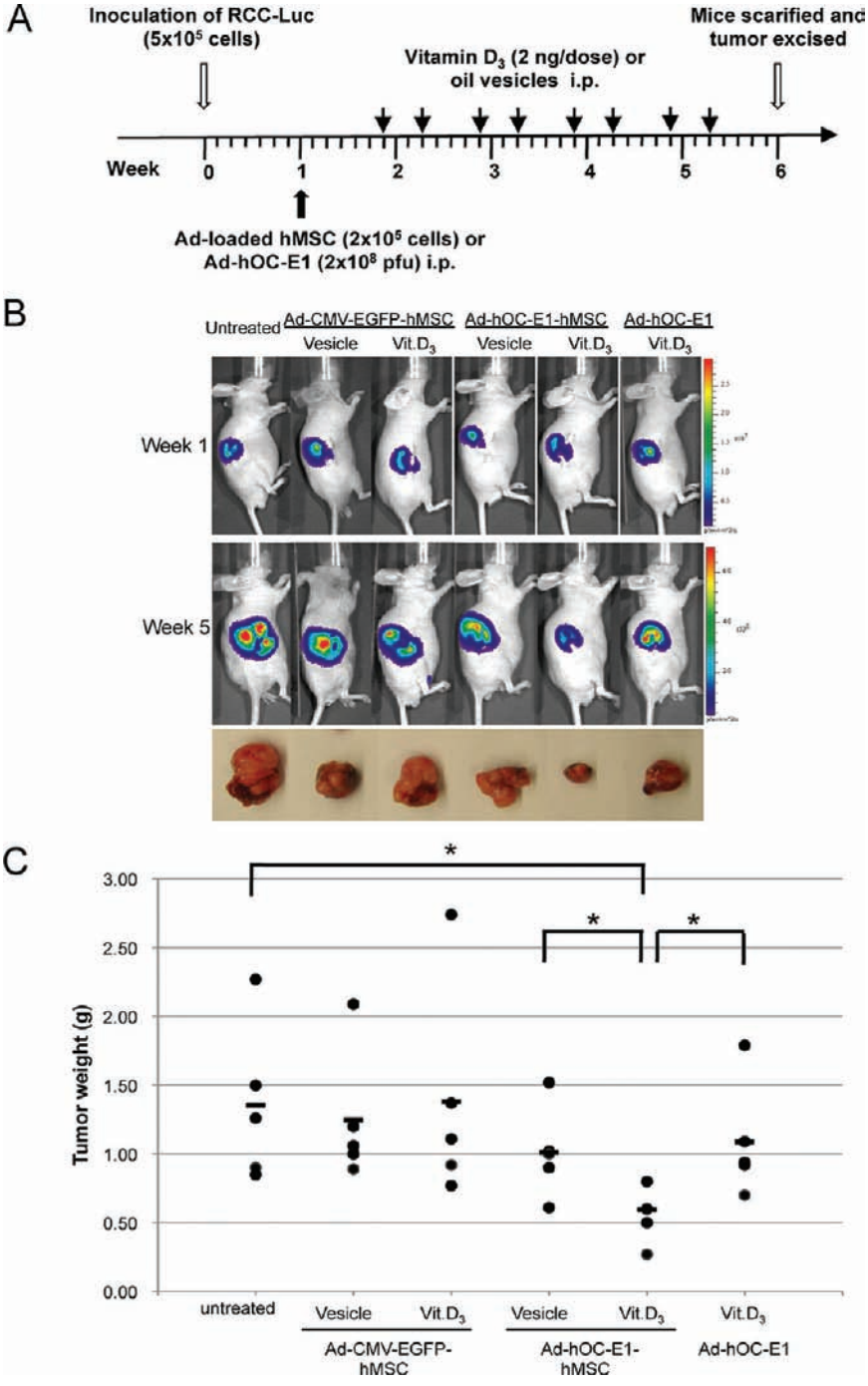

Figure 6. Antitumor effect of the combined treatment of Ad-hOC-E1-loaded hMSC and vitamin D_3 in mice with orthotopic RCC tumors. (A) Experimental scheme. As described in Materials and Methods, tumor-bearing mice were treated i.p. with a single dose of 2×10^5 hMSCs infected with Ad-hOC-E1- or Ad-CMV-EGFP-(moi 1000) or 2×10^8 pfu of carrier-free Ad-hOC-E1 viruses on week 1 after RCC-Luc inoculation. Six days later mice were given i.p. vitamin D_3 (2 ng/dose) or oil vehicle twice per week for 4 weeks. Mice were sacrificed, and tumors were excised for evaluation on week 6. (B) Representative bioluminescence images from control and treated animals before (week 1) and after (week 5) treatment. Tumors were excised at the end of treatment and are displayed below the corresponding animals. (C) Wet weight of individual tumors. Bars indicate the mean tumor weights for each group (n = 5 mice per group; *, $p < 0.05$ one-way ANOVA).

We further examined the pathologic changes in tumors treated with the combination of Ad-hOC-E1-loaded hMSC and vitamin D_3 and compared the results with other treatment groups. Histological analysis (Figure 7, H&E) revealed healthy and packed tumor cells in the control group of either no-treatment or treated with Ad-CMV-EGFP-loaded hMSC, whereas large necrotic regions were found in tumors excised from the Ad-hOC-E1-loaded hMSCs plus vitamin D_3 treated animals. In the group of Ad-hOC-E1-loaded hMSCs alone or carrier-free i.p. Ad-hOC-E1 viral injection combined with vitamin D_3, only small focal areas of necrosis were noted in tumor tissues. Around the necrotic areas, a significant positive staining for adenovirus capsid protein hexon was observed in Ad-hOC-E1-loaded hMSC plus vitamin D_3 treatment group (Figure 7, Hexon), indicating an active viral replication within the tumors. In additional, the *in situ* cell death assay (Figure 7,

dx.doi.org/10.1021/mp200649g | *Mol. Pharmaceutics* 2012, 9, 1396–1408

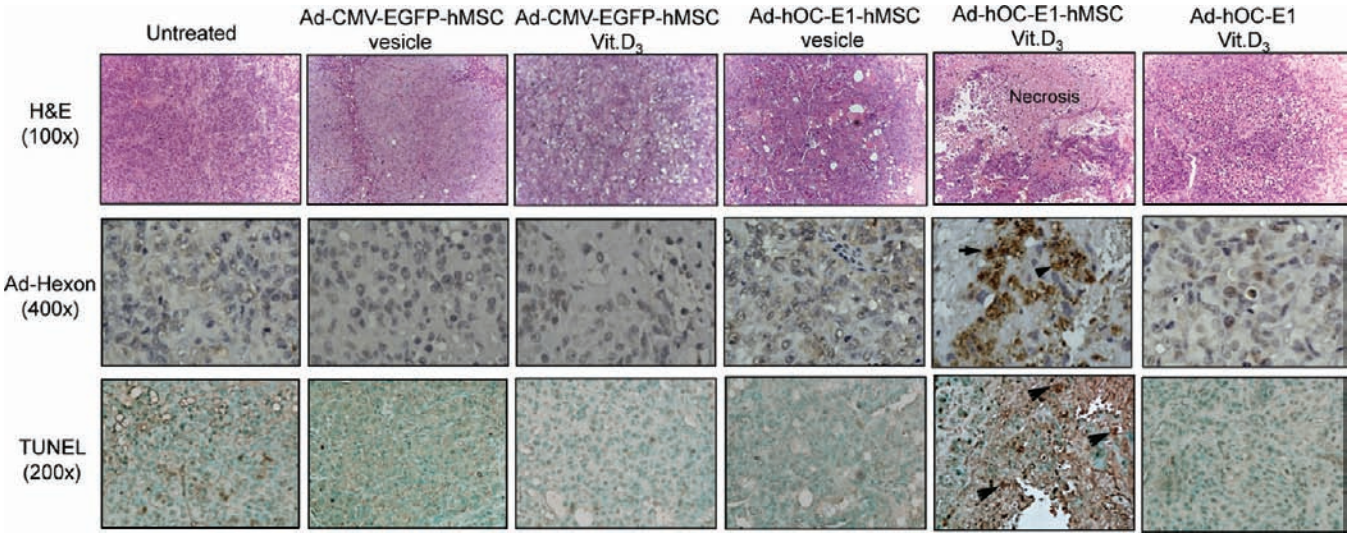

Figure 7. Histopathologic examination of RCC xenograft tumors. Validation of regression of RCC xenografts by histopathological analysis (hematoxylin and eosin staining: H&E). Immunostaining of adenoviral hexon antigen (Ad-Hexon; arrows) shows production of adenoviral particles after treatment. Increased apoptosis was determined by TUNEL-positive cells (dark brown reaction product, arrowhead).

TUNEL) also showed an abundance of TUNEL positive cells in these tumor sections, suggesting a strong apoptotic response had occurred in the Ad-hOC-E1-loaded hMSC/vitamin D_3 combination therapy. In other treatment regimens, weak and sporadically positive staining for hexon was found in tumors from the group of Ad-hOC-E1-loaded hMSC treated alone and the i.p. injection of carrier-free Ad-hOC-E1 virus combined with vitamin D_3, but no evidence of hexon protein expression was detected in either the untreated or Ad-CMV-EGFP-loaded hMSC control group. Taken together, these results demonstrated a vitamin D_3-inducible and hMSC carrier-dependent antitumor effect of oncolytic Ad-hOC-E1 therapy for RCC.

■ DISCUSSION

To date, only one report described the application of MSCs to track and deliver therapeutic agents to human RCC, which was demonstrated in a mouse model of subcutaneous RCC xenografts.[23] Heterotopic tumor models where the tumor growing microenvironment is not relevant to that of primary and metastatic disease are currently considered inappropriate use for the study of human tumors.[24] In the present study, we developed an orthotopic tumor model in which RCC cells were implanted into the renal subcapsule to develop fast-growing tumors in the kidney. This model thus has higher clinical relevance over subcutaneous mouse models for preclinical evaluation of cell carrier-based RCC tumor targeting. Although the risk of seminal vesicle metastasis of human RCC is relatively low by clinical observation,[25−27] using luciferase-tagged hMSC cells as a noninvasive imaging modality, we clearly showed that i.p. administered hMSC cells progressively and preferentially localized in orthotopic RCC tumors and their developed seminal vesicle metastases. To our knowledge, this is the first report of the inherent ability of hMSCs for tracking primary and disseminated RCC cells in orthotopic mouse models. However, we are also aware that tumor-tropic migration of transplanted hMSCs seems to be dependent on the experimental route of administration since intravenously administered hMSCs remained trapped in the lung and failed to migrate into the RCC tumors (data not shown). It has been suggested that the larger size of MSCs than the size of pulmonary capillaries causes intravenously injected MSCs trapped in the lung and prevents the cells access to other organs.[28] Intraperitoneal delivery thus might be a better option to MSC-based therapy for compared to intravenous administration as it bypasses the filtering organs. This observation has to be taken into consideration when designing preclinical or clinical trials for tumors from different anatomical locations.

PDGF-AA is recognized as a key regulator in directional cell migration during embryonic development[29] and a potent chemoattractant for human monocytes, granulocytes, and skin fibroblasts.[30,31] However, the paracrine effect of tumor-derived PDGF-AA on MSC homing has not been explored previously. In this study, we found that RCC cell lines in general express high levels of PDGF-AA. PDGF-AA levels correlated with the clinical status of patients as overexpression of PDGF-AA is identified in grades 3 and 4 RCC and is associated with an adverse outcome.[32] In addition, our results showed that RCC-conditioned medium and purified PDGF-AA induced a significant migratory response of hMSCs, and this RCC-induced chemotaxis was significantly inhibited after depletion of PDGF-AA from conditioned medium; these findings identify a new action of PDGF-AA as an RCC-specific chemotactic factor for MSC tumor tropism. Although not the primary focus of the present study, we found that coculturing hMSCs and RCC cells has no effect on RCC cell proliferation but increased their migratory ability and invasiveness *in vitro* (data not shown). This result agrees with other findings from breast cancer,[33,34] prostate cancer,[35] and colon cancer[36] that MSCs promote tumor development and progression and implicates a role of MSCs on RCC tumor metastasis. Since sutent (sunitinib) inhibits phosphorylation of PDGFR, interrupts angiogenesis and cell proliferation,[37] and is approved for the treatment of metastatic RCC, our findings of overexpression of the corresponding receptor of PDGF-AA, PDGFRα, on hMSCs may provide an additional mechanistic basis for these agents as novel therapeutic approaches against cancer.

Besides tumor localization, our *in vivo* kinetics study revealed that freely circulating hMSCs were retained in the abdominal cavity for 3 days before engrafting into the tumor microenvironment. As cell lysis and releasing progeny adenoviral

particles occur 24−48 h after infection, this result pointed out the efficacy and safety issues of uncontrollable hMSC-based oncolytic virotherapy by their early release of viruses into the circulation. The most promising strategy to target the oncolytic activity of adenoviruses only at tumor cells but not harm normal tissues is to use tumor-specific promoters, which have been widely applied in clinical trials.[38] However, these formats of conditionally replicating adenoviruses cannot be adopted with cell-based delivery since their tumor-specific promoters were originally designed to be silent in noncancerous cells. The osteoblast-specific OC gene was recently demonstrated to be also expressed by osteotropic cancers, including lung, brain, and prostate, and kidney cancers,[5,39] which has led to the development of OC promoters as a tissue-specific and tumor-restricted promoter to cotarget both tumor epithelial and their supporting osteoblasts for better control of cancer bone metastases.[18,40] In the present study, we further demonstrated the ability of vitamin D_3 analogues to induce OC gene as well as hOC-promoter-driven transgene expression in hMSCs, which results in enhanced therapeutic effect of oncolytic Ad-hOC-E1 on RCC. The effective and timely control of amplification of the initial adenoviral vectors loaded in the hMSC carriers provides additional advantages of using vitamin D_3-inducible OC promoter over other currently developed promoters either ubiquitously active or cell-specific expression for MSC-delivered oncolytic virotherapy. Although complete tumor regression was not achieved by current format of these agents, cell-based therapy can be enhanced by engineered targeting via expressing receptors critical to the migratory competence of cell carriers to tumors.[41,42] Since PDGF-AA only stimulates PDGFR-$\alpha\alpha$, ectopically overexpressing PDGFR-$\alpha\alpha$ in the cell membrane of hMSCs may maximize cell vehicle concentration at the target location and improve the therapeutic value of the overall system.

In summary, in the present study, we have evaluated the potential utility of hMSC-mediated delivery of a vitamin D_3-controlled oncolytic adenoviral therapy for systemic treatment of advanced RCC, which has not been described hitherto. Currently, clinical trials using MSCs for the regeneration of soft tissue, craniofacial tissue, and cardiovascular tissue have enrolled a number of patients. Unlike embryonic stem cells, MSCs can be isolated as a fraction of bone marrow cells or other adult tissues and expanded in culture, thus posing no ethical conflicts when used for therapeutic regiments. In addition, osteocalcin promoter-directed gene therapy using adenoviral vectors is undergoing clinical trials for targeting metastatic prostate cancer.[43−45] Vitamin D_3 is in a FDA-approved nutritional supplement used for cancer prevention and treatment.[46,47] This specific and directed approach therefore could move rapidly from preclinical development to the clinic by using agents that have been approved for clinical trials. The hMSC-mediated delivery of a vitamin D_3-controlled oncolytic adenoviral therapy holds enormous potential for systemic treatment of patients suffering from advanced RCC. The immune response against viral vectors is one of the major hurdles in the clinical application of the oncolytic viral therapy. Bone marrow-derived MSCs have been shown to enhance intratumoral persistence of oncolytic adenoviruses by suppressing T lymphocyte activation and antiviral cytokine production.[48] Further evaluation of the distribution, tolerability, and efficacy of MSC-delivered Ad-hOC-E1 in a murine model with preexisting humoral immunity similar to humans will support the translation of these experimental findings to the clinical setting.

■ ASSOCIATED CONTENT

Supporting Information

Additional figures as discussed in the manuscript. This material is available free of charge via the Internet at http://pubs.acs.org.

■ AUTHOR INFORMATION

Corresponding Author

*China Medical University Hospital, Center for Molecular Medicine, 9F, No. 6, Hsueh-Shih Road, Taichung 40454, Taiwan. E-mail: chsieh2@mail.cmu.edu.tw. Telephone: +886-4-22052121 ext. 7923. Fax: +886-4-22333496.

Author Contributions

†These authors contributed equally to this article.

Notes

The authors declare no competing financial interest.

■ ACKNOWLEDGMENTS

We thank MedcomAsia for their editorial assistance. This work was supported by NSC 100-3122-B-039-005, NSC 99-2320-B-039-029-MY3, and NSC 99-2632-B-039-001-MY3 from the National Science Council and NHRI EX-100-9902BI from the National Health Research Institutes in Taiwan.

■ REFERENCES

(1) Motzer, R. J.; Bander, N. H.; Nanus, D. M. Renal-cell carcinoma. *N. Engl. J. Med.* **1996**, *335* (12), 865−75.

(2) Campbell, S. C.; Flanigan, R. C.; Clark, J. I. Nephrectomy in metastatic renal cell carcinoma. *Curr. Treat. Options Oncol.* **2003**, *4* (5), 363−72.

(3) Powles, T.; Chowdhury, S.; Jones, R.; Mantle, M.; Nathan, P.; Bex, A.; Lim, L.; Hutson, T. Sunitinib and other targeted therapies for renal cell carcinoma. *Br. J. Cancer* **2011**, *104* (5), 741−5.

(4) Huang, P.; Kaku, H.; Chen, J.; Kashiwakura, Y.; Saika, T.; Nasu, Y.; Urata, Y.; Fujiwara, T.; Watanabe, M.; Kumon, H. Potent antitumor effects of combined therapy with a telomerase-specific, replication-competent adenovirus (OBP-301) and IL-2 in a mouse model of renal cell carcinoma. *Cancer Gene Ther.* **2010**, *17* (7), 484−91.

(5) Johnson, N. A.; Chen, B. H.; Sung, S. Y.; Liao, C. H.; Hsiao, W. C.; Chung, L. W. K.; Hsieh, C.-L. A novel targeting modality for renal cell carcinoma: human osteocalcin promoter-mediated gene therapy synergistically induced by vitamin C and vitamin D. *J. Gene Med.* **2010**, *12* (11), 892−903.

(6) Heise, C.; Sampson-Johannes, A.; Williams, A.; McCormick, F.; Von Hoff, D. D.; Kirn, D. H. ONYX-015, an E1B gene-attenuated adenovirus, causes tumor-specific cytolysis and antitumoral efficacy that can be augmented by standard chemotherapeutic agents. *Nat. Med.* **1997**, *3* (6), 639−45.

(7) DeWeese, T. L.; van der Poel, H.; Li, S.; Mikhak, B.; Drew, R.; Goemann, M.; Hamper, U.; DeJong, R.; Detorie, N.; Rodriguez, R.; Haulk, T.; DeMarzo, A. M.; Piantadosi, S.; Yu, D. C.; Chen, Y.; Henderson, D. R.; Carducci, M. A.; Nelson, W. G.; Simons, J. W. A phase I trial of CV706, a replication-competent, PSA selective oncolytic adenovirus, for the treatment of locally recurrent prostate cancer following radiation therapy. *Cancer Res.* **2001**, *61* (20), 7464−72.

(8) Yu, D. C.; Chen, Y.; Dilley, J.; Li, Y.; Embry, M.; Zhang, H.; Nguyen, N.; Amin, P.; Oh, J.; Henderson, D. R. Antitumor synergy of CV787, a prostate cancer-specific adenovirus, and paclitaxel and docetaxel. *Cancer Res.* **2001**, *61* (2), 517−25.

(9) Liu, T. C.; Galanis, E.; Kirn, D. Clinical trial results with oncolytic virotherapy: a century of promise, a decade of progress. *Nat. Clin. Pract. Oncol.* **2007**, *4* (2), 101−17.
(10) Studeny, M.; Marini, F. C.; Dembinski, J. L.; Zompetta, C.; Cabreira-Hansen, M.; Bekele, B. N.; Champlin, R. E.; Andreeff, M. Mesenchymal stem cells: potential precursors for tumor stroma and targeted-delivery vehicles for anticancer agents. *J. Natl. Cancer Inst.* **2004**, *96* (21), 1593−603.
(11) Hall, B.; Andreeff, M.; Marini, F. The participation of mesenchymal stem cells in tumor stroma formation and their application as targeted-gene delivery vehicles. *Handb. Exp. Pharmacol.* **2007**, No. 180, 263−83.
(12) Roorda, B. D.; ter Elst, A.; Kamps, W. A.; de Bont, E. S. Bone marrow-derived cells and tumor growth: contribution of bone marrow-derived cells to tumor micro-environments with special focus on mesenchymal stem cells. *Crit. Rev. Oncol. Hematol.* **2009**, *69* (3), 187−98.
(13) Stoff-Khalili, M. A.; Rivera, A. A.; Mathis, J. M.; Banerjee, N. S.; Moon, A. S.; Hess, A.; Rocconi, R. P.; Numnum, T. M.; Everts, M.; Chow, L. T.; Douglas, J. T.; Siegal, G. P.; Zhu, Z. B.; Bender, H. G.; Dall, P.; Stoff, A.; Pereboeva, L.; Curiel, D. T. Mesenchymal stem cells as a vehicle for targeted delivery of CRAds to lung metastases of breast carcinoma. *Br. Cancer Res. Treat.* **2007**, *105* (2), 157−67.
(14) Yong, R. L.; Shinojima, N.; Fueyo, J.; Gumin, J.; Vecil, G. G.; Marini, F. C.; Bogler, O.; Andreeff, M.; Lang, F. F. Human bone marrow-derived mesenchymal stem cells for intravascular delivery of oncolytic adenovirus Delta24-RGD to human gliomas. *Cancer Res.* **2009**, *69* (23), 8932−40.
(15) Sonabend, A. M.; Ulasov, I. V.; Tyler, M. A.; Rivera, A. A.; Mathis, J. M.; Lesniak, M. S. Mesenchymal stem cells effectively deliver an oncolytic adenovirus to intracranial glioma. *Stem Cells* **2008**, *26* (3), 831−41.
(16) Komarova, S.; Kawakami, Y.; Stoff-Khalili, M. A.; Curiel, D. T.; Pereboeva, L. Mesenchymal progenitor cells as cellular vehicles for delivery of oncolytic adenoviruses. *Mol. Cancer Ther.* **2006**, *5* (3), 755−66.
(17) Weber, W.; Fussenegger, M. Pharmacologic transgene control systems for gene therapy. *J. Gene Med.* **2006**, *8* (5), 535−56.
(18) Hsieh, C. L.; Yang, L.; Miao, L.; Yeung, F.; Kao, C.; Yang, H.; Zhau, H. E.; Chung, L. W. A novel targeting modality to enhance adenoviral replication by vitamin D(3) in androgen-independent human prostate cancer cells and tumors. *Cancer Res.* **2002**, *62* (11), 3084−92.
(19) Liu, P.; Oyajobi, B. O.; Russell, R. G.; Scutt, A. Regulation of osteogenic differentiation of human bone marrow stromal cells: interaction between transforming growth factor-beta and 1,25(OH)(2) vitamin D(3) In vitro. *Calcif. Tissue Int.* **1999**, *65* (2), 173−80.
(20) Jin, F.; Xie, Z.; Kuo, C. J.; Chung, L. W.; Hsieh, C. L. Cotargeting tumor and tumor endothelium effectively inhibits the growth of human prostate cancer in adenovirus-mediated antiangiogenesis and oncolysis combination therapy. *Cancer Gene Ther.* **2005**, *12* (3), 257−67.
(21) Hung, S. C.; Wu, I. H.; Hsue, S. S.; Liao, C. H.; Wang, H. C.; Chuang, P. H.; Sung, S. Y.; Hsieh, C. L. Targeting l1 cell adhesion molecule using lentivirus-mediated short hairpin RNA interference reverses aggressiveness of oral squamous cell carcinoma. *Mol. Pharmaceutics* **2010**, *7* (6), 2312−23.
(22) Yeung, F.; Law, W. K.; Yeh, C. H.; Westendorf, J. J.; Zhang, Y.; Wang, R.; Kao, C.; Chung, L. W. Regulation of human osteocalcin promoter in hormone-independent human prostate cancer cells. *J. Biol. Chem.* **2002**, *277* (4), 2468−76.
(23) Gao, P.; Ding, Q.; Wu, Z.; Jiang, H.; Fang, Z. Therapeutic potential of human mesenchymal stem cells producing IL-12 in a mouse xenograft model of renal cell carcinoma. *Cancer Lett.* **2010**, *290* (2), 157−66.
(24) Killion, J. J.; Radinsky, R.; Fidler, I. J. Orthotopic models are necessary to predict therapy of transplantable tumors in mice. *Cancer Metastasis Rev.* **1998**, *17* (3), 279−84.
(25) Matsuzaki, K.; Yasunaga, Y.; Fukuda, S.; Oka, T. Seminal vesicle metastasis of renal cell carcinoma. *Urology* **2009**, *74* (5), 1017−8.
(26) Yamamoto, S.; Mamiya, Y.; Noda, K.; Samejima, T.; Miki, M.; Akasaka, Y. A case of metastasis to the seminal vesicle of renal cell carcinoma. *Nihon Hinyokika Gakkai Zasshi* **1998**, *89* (5), 563−6.
(27) Reisman, Y.; de Reijke, T. M. An unusual cause of irritable urinary bladder symptoms. *Urol. Int.* **2001**, *66* (4), 225−6.
(28) Schrepfer, S.; Deuse, T.; Reichenspurner, H.; Fischbein, M. P.; Robbins, R. C.; Pelletier, M. P. Stem cell transplantation: the lung barrier. *Transplant. Proc.* **2007**, *39* (2), 573−6.
(29) Hoch, R. V.; Soriano, P. Roles of PDGF in animal development. *Development* **2003**, *130* (20), 4769−84.
(30) Shure, D.; Senior, R. M.; Griffin, G. L.; Deuel, T. F. PDGF AA homodimers are potent chemoattractants for fibroblasts and neutrophils, and for monocytes activated by lymphocytes or cytokines. *Biochem. Biophys. Res. Commun.* **1992**, *186* (3), 1510−4.
(31) Soma, Y.; Mizoguchi, M.; Yamane, K.; Yazawa, N.; Kubo, M.; Ihn, H.; Kikuchi, K.; Tamaki, K. Specific inhibition of human skin fibroblast chemotaxis to platelet-derived growth factor A-chain homodimer by transforming growth factor-beta1. *Arch. Dermatol. Res.* **2002**, *293* (12), 609−13.
(32) Sulzbacher, I.; Birner, P.; Traxler, M.; Marberger, M.; Haitel, A. Expression of platelet-derived growth factor-alpha alpha receptor is associated with tumor progression in clear cell renal cell carcinoma. *Am. J. Clin. Pathol.* **2003**, *120* (1), 107−12.
(33) Rhodes, L. V.; Muir, S. E.; Elliott, S.; Guillot, L. M.; Antoon, J. W.; Penfornis, P.; Tilghman, S. L.; Salvo, V. A.; Fonseca, J. P.; Lacey, M. R.; Beckman, B. S.; McLachlan, J. A.; Rowan, B. G.; Pochampally, R.; Burow, M. E. Adult human mesenchymal stem cells enhance breast tumorigenesis and promote hormone independence. *Br. Cancer Res. Treat.* **2010**, *121* (2), 293−300.
(34) Karnoub, A. E.; Dash, A. B.; Vo, A. P.; Sullivan, A.; Brooks, M. W.; Bell, G. W.; Richardson, A. L.; Polyak, K.; Tubo, R.; Weinberg, R. A. Mesenchymal stem cells within tumour stroma promote breast cancer metastasis. *Nature* **2007**, *449* (7162), 557−63.
(35) Placencio, V. R.; Li, X.; Sherrill, T. P.; Fritz, G.; Bhowmick, N. A. Bone marrow derived mesenchymal stem cells incorporate into the prostate during regrowth. *PLoS ONE* **2010**, *5* (9), e12920.
(36) Shinagawa, K.; Kitadai, Y.; Tanaka, M.; Sumida, T.; Kodama, M.; Higashi, Y.; Tanaka, S.; Yasui, W.; Chayama, K. Mesenchymal stem cells enhance growth and metastasis of colon cancer. *Int. J. Cancer* **2010**, *127* (10), 2323−33.
(37) Motzer, R. J.; Hutson, T. E.; Tomczak, P.; Michaelson, M. D.; Bukowski, R. M.; Rixe, O.; Oudard, S.; Negrier, S.; Szczylik, C.; Kim, S. T.; Chen, I.; Bycott, P. W.; Baum, C. M.; Figlin, R. A. Sunitinib versus interferon alfa in metastatic renal-cell carcinoma. *N. Engl. J. Med.* **2007**, *356* (2), 115−24.
(38) Ko, D.; Hawkins, L.; Yu, D. C. Development of transcriptionally regulated oncolytic adenoviruses. *Oncogene* **2005**, *24* (52), 7763−74.
(39) Koeneman, K. S.; Kao, C.; Ko, S. C.; Yang, L.; Wada, Y.; Kallmes, D. F.; Gillenwater, J. Y.; Zhau, H. E.; Chung, L. W.; Gardner, T. A. Osteocalcin-directed gene therapy for prostate-cancer bone metastasis. *World J. Urol.* **2000**, *18* (2), 102−10.
(40) Matsubara, S.; Wada, Y.; Gardner, T. A.; Egawa, M.; Park, M. S.; Hsieh, C. L.; Zhau, H. E.; Kao, C.; Kamidono, S.; Gillenwater, J. Y.; Chung, L. W. A conditional replication-competent adenoviral vector, Ad-OC-E1a, to cotarget prostate cancer and bone stroma in an experimental model of androgen-independent prostate cancer bone metastasis. *Cancer Res.* **2001**, *61* (16), 6012−9.
(41) Sato, H.; Kuwashima, N.; Sakaida, T.; Hatano, M.; Dusak, J. E.; Fellows-Mayle, W. K.; Papworth, G. D.; Watkins, S. C.; Gambotto, A.; Pollack, I. F.; Okada, H. Epidermal growth factor receptor-transfected bone marrow stromal cells exhibit enhanced migratory response and therapeutic potential against murine brain tumors. *Cancer Gene Ther.* **2005**, *12* (9), 757−68.
(42) Komarova, S.; Roth, J.; Alvarez, R.; Curiel, D. T.; Pereboeva, L. Targeting of mesenchymal stem cells to ovarian tumors via an artificial receptor. *J. Ovarian Res.* **2010**, *3*, 12.

(43) Shirakawa, T.; Terao, S.; Hinata, N.; Tanaka, K.; Takenaka, A.; Hara, I.; Sugimura, K.; Matsuo, M.; Hamada, K.; Fuji, K.; Okegawa, T.; Higashihara, E.; Gardner, T. A.; Kao, C.; Chung, L. W.; Kamidono, S.; Fujisawa, M.; Gotoh, A. Long-term outcome of phase I/II clinical trial of Ad-OC-TK/VAL gene therapy for hormone-refractory metastatic prostate cancer. *Hum. Gene Ther.* **2007**, *18* (12), 1225−32.
(44) Hinata, N.; Shirakawa, T.; Terao, S.; Goda, K.; Tanaka, K.; Yamada, Y.; Hara, I.; Kamidono, S.; Fujisawa, M.; Gotoh, A. Progress report on phase I/II clinical trial of Ad-OC-TK plus VAL therapy for metastatic or locally recurrent prostate cancer: Initial experience at Kobe University. *Int. J. Urol.* **2006**, *13* (6), 834−7.
(45) Kubo, H.; Gardner, T. A.; Wada, Y.; Koeneman, K. S.; Gotoh, A.; Yang, L.; Kao, C.; Lim, S. D.; Amin, M. B.; Yang, H.; Black, M. E.; Matsubara, S.; Nakagawa, M.; Gillenwater, J. Y.; Zhau, H. E.; Chung, L. W. Phase I dose escalation clinical trial of adenovirus vector carrying osteocalcin promoter-driven herpes simplex virus thymidine kinase in localized and metastatic hormone-refractory prostate cancer. *Hum. Gene Ther.* **2003**, *14* (3), 227−41.
(46) Lappe, J. M.; Travers-Gustafson, D.; Davies, K. M.; Recker, R. R.; Heaney, R. P. Vitamin D and calcium supplementation reduces cancer risk: results of a randomized trial. *Am. J. Clin. Nutr.* **2007**, *85* (6), 1586−91.
(47) Schwartz, G. G. Vitamin D and intervention trials in prostate cancer: from theory to therapy. *Ann. Epidemiol.* **2009**, *19* (2), 96−102.
(48) Ahmed, A. U.; Rolle, C. E.; Tyler, M. A.; Han, Y.; Sengupta, S.; Wainwright, D. A.; Balyasnikova, I. V.; Ulasov, I. V.; Lesniak, M. S. Bone marrow mesenchymal stem cells loaded with an oncolytic adenovirus suppress the anti-adenoviral immune response in the cotton rat model. *Mol. Ther.* **2010**, *18* (10), 1846−56.